Application of metabolic controls for the maximization of lipid production in semicontinuous fermentation

Jingyang Xu[a,b], Nian Liu[a], Kangjian Qiao[a], Sebastian Vogg[a], and Gregory Stephanopoulos[a,1]

[a]Department of Chemical Engineering, Massachusetts Institute of Technology, Cambridge, MA 02139; and [b]Department of Forensic Science and Technology, Zhejiang Police College, Hangzhou 310053, China

Edited by Harvey W. Blanch, University of California, Berkeley, CA, and accepted by Editorial Board Member James A. Dumesic May 22, 2017 (received for review March 6, 2017)

Acetic acid can be generated through syngas fermentation, lignocellulosic biomass degradation, and organic waste anaerobic digestion. Microbial conversion of acetate into triacylglycerols for biofuel production has many advantages, including low-cost or even negative-cost feedstock and environmental benefits. The main issue stems from the dilute nature of acetate produced in such systems, which is costly to be processed on an industrial scale. To tackle this problem, we established an efficient bioprocess for converting dilute acetate into lipids, using the oleaginous yeast *Yarrowia lipolytica* in a semicontinuous system. The implemented design used low-strength acetic acid in both salt and acid forms as carbon substrate and a cross-filtration module for cell recycling. Feed controls for acetic acid and nitrogen based on metabolic models and online measurement of the respiratory quotient were used. The optimized process was able to sustain high-density cell culture using acetic acid of only 3% and achieved a lipid titer, yield, and productivity of 115 g/L, 0.16 g/g, and 0.8 g·L^{-1}·h^{-1}, respectively. No carbon substrate was detected in the effluent stream, indicating complete utilization of acetate. These results represent a more than twofold increase in lipid production metrics compared with the current best-performing results using concentrated acetic acid as carbon feed.

lipid production | acetate | tangential filtration | dynamic modeling | exhaust gas analysis

The development of biofuels has largely been driven by dwindling petroleum reserves and major environmental concerns. As an alternative fuel source, environmentally friendly liquid biofuels derived from gaseous substrates have garnered much interest. In this process, mixtures of CO_2, CO, and H_2 are converted biologically and renewably, via an acetic acid intermediate, to liquid fuels [biogas to liquids (bio-GTL)] (Fig. 1) (1). Syngas constitutes one of the major feedstocks for this platform due to its high availability, with global capacity being 154 Gigawatts thermal (GWth) currently and predicted to reach about 370 GWth by 2020 (2). Gasification of biomass and organic waste (3), recycling of industrial off-gases (4), and thermochemical dissociation of CO_2 and H_2O using solar energy (5) will also be available to provide plentiful amounts of renewable syngas. By using the Wood–Ljungdahl pathway, acetogenic bacteria are able to convert the syngas into acetic acid as the main product (6, 7). Additionally, as the key intermediate in this process, acetic acid can also be generated renewably from other sources, expanding the range of feedstocks that can drive bio-GTL operation. Examples include conversion of lignocellulosic biomass and municipal solid waste (MSW) into acetic acid through pyrolysis (8) and anaerobic fermentation (9), respectively, both of which contribute no net carbon into the ecosystem. In a second step, the acetate generated from these various sources can be further upgraded biologically into a variety of liquid fuels and value-added chemicals. In particular, oleaginous microorganisms can produce medium- and long-chain triacylglycerols for biodiesel preparation. Currently the best reported results for this step were produced using an engineered *Yarrowia lipolytica* strain with the cofeeding of concentrated and dilute acetate under nitrogen starvation conditions, resulting in a yield, titer, and productivity of 0.16 g/g, 46 g/L, and 0.27 g·L^{-1}·h^{-1}, respectively (10, 11). Overall, the bio-GTL platform (Fig. 1) that generates liquid biofuels from a variety of starting feedstocks offers several key advantages, including mild operating conditions, high tolerance to gas impurities, low or even negative feedstock costs, and, in some cases, zero carbon emission or net carbon fixation (12, 13). Therefore, the development of this platform is essential in realizing an industrial process that can partially alleviate our reliance on petroleum in the short term and build toward a clean energy infrastructure in the future.

One of the most challenging objectives in the present scheme is the efficient utilization of low-strength acetic acid obtained from acetogenesis and biomass/MSW degradation, which is typically below 2∼3% (20∼30 g/L) (9, 14). Substrates with low concentrations are difficult to process biologically because large feed volumes are required. We estimate that for every 100 g of lipids synthesized, more than 20 L of 3% acetic acid needs to be fed, which is beyond the typical operation capacity of a conventional lipid production process under batch or fed-batch modes (15–18). Moreover, improper feeding of dilute substrates can easily cause nutrient starvation and inhibit cell metabolism. One obvious approach to resolve this issue would be to concentrate acetic acid before lipid conversion. However, concentration of dilute acetic acid would introduce high costs at an industrial scale (3, 19). Furthermore, the use of concentrated acetic acid in a fermentation process may result in significant carbon losses due to incomplete consumption by the cells and

Significance

This work establishes a semicontinuous process for efficient and complete upgrading of low-strength acetic acid into lipids. By implementing control strategies in response to the time-varying nature of cell metabolism, we achieved and sustained lipid yields close to the theoretical maximum while maintaining high productivities. The control algorithm was designed to respond to readily available real-time measurements and basic principles, which is ideal for industrial applications. Overall, our process scheme can directly take in dilute nutrient streams that are difficult and costly to purify and is able to biologically convert them into highly concentrated value-added products. This design significantly reduces the energy costs associated with processes using dilute feedstocks, which typically require initial concentration of the feed.

Author contributions: J.X. and G.S. designed research; J.X. performed research; J.X., N.L., K.Q., and S.V. analyzed data; and J.X., N.L., and G.S. wrote the paper.

The authors declare no conflict of interest.

This article is a PNAS Direct Submission. H.W.B. is a guest editor invited by the Editorial Board.

[1]To whom correspondence should be addressed. Email: gregstep@mit.edu.

This article contains supporting information online at www.pnas.org/lookup/suppl/doi:10.1073/pnas.1703321114/-/DCSupplemental.

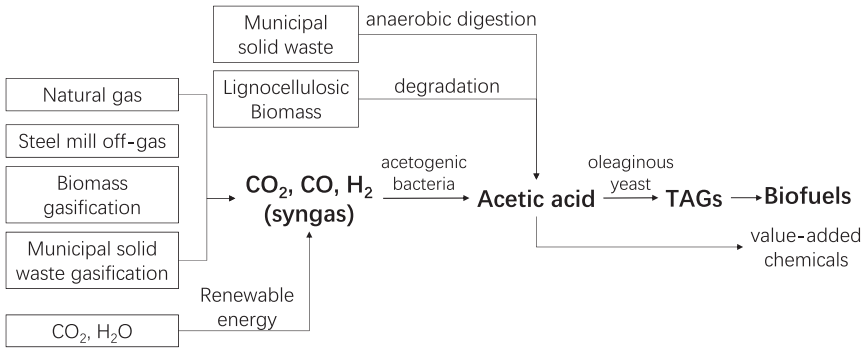

Fig. 1. Integrated bio-GTL platform. Syngas can be derived from a variety of low- or even negative-cost feedstocks. However, syngas by itself is not an ideal fuel source due to many issues such as low energy density, difficulty to transport across large distances, and potential safety hazards as a flammable gas. In this platform, it can be biologically upgraded, via an acetic acid intermediate, into liquid fuels and other value-added chemicals. Abbreviations used: TAG, triacylglyceride.

generation of by-products due to excessive carbon flux through undesired pathways (11). Consequently, with these considerations in mind, we believe that the engineering of a bioprocess that can produce lipids at high yield, titer, and productivity from dilute acetate streams only is paramount in overcoming this bottleneck in the bio-GTL conversion scheme.

Herein, we demonstrate a cell recycle process that can efficiently generate lipids with high production metrics, using only low-strength acetic acid. A semicontinuous fermenter was established with a tangential filtration module, which continuously enriched lipid products along with yeast cells while removing extra volumes of feed liquid from the permeate. In addition, instead of applying the "carbon-rich and nitrogen starvation" strategy, we used a "carbon-restrained" mode, using a joint feed of acetic acid in both the acid and the salt forms. The goal of this operation mode was to achieve zero acetate concentration in the fermentation broth without starving the cells, thereby ensuring minimal carbon loss from the effluent while still obtaining high productivities. An initial control scheme for the feeding streams was formulated based on fermentation models, which determined feed strategies intermittently by incorporating data from off-line measurements including cell density, substrate concentration, permeate volume, etc. The algorithm was then improved to perform real-time calculations built upon on-line pH measurements only. This approach enhanced the accuracy of carbon feed control and resulted in accelerated lipid production. Finally, based on real-time respiratory quotient analysis, a closed-loop control for nitrogen feed was also integrated into the algorithm. The final optimized control model offered both carbon and nitrogen feed strategies to operate dynamically, synchronizing with the time-varying nature of cell metabolism. This design allowed us to achieve superior lipid titer and productivity (115 g/L and 0.8 $g{\cdot}L^{-1}{\cdot}h^{-1}$, respectively), which represents more than 150% improvement over the current best-performing results using only low-strength acetic acid as the carbon feed.

Results and Discussion

Lipid Production Under a Carbon-Restrained Mode by Feeding Dilute Acetic Acid. A cell recycling system allowed the accumulation of biomass together with its intracellular lipid product in the reactor while the excess volume (mostly water) from the feed liquid was removed simultaneously, enabling the utilization of large volumes of low-strength acetic acid. The process flowchart is depicted in Fig. S1. However, in such a semicontinuous fermentation system, the widely applied "carbon-rich" mode (maintaining a relatively high carbon concentration to that of nitrogen such that the excess carbon can lead to lipid synthesis in *Y. lipolytica*) results in significant carbon loss through the permeate of the cross flow filter. To avoid this, acetic acid should be fed continuously but its concentration within the reactor needs to be maintained near zero such that the carbons can be fully used for cell growth, lipid synthesis, and maintaining cellular function instead of being discharged through the permeate. Note that this concept of "carbon-restrained mode" differs from "carbon-limited mode" in that the cells should not be starved due to limited carbon supply.

To determine the optimal method for dilute acetic acid feeding that achieves such an operation mode, we first cultured *Y. lipolytica* by feeding 3% dilute acetic acid (30 g/L), which is a typical output concentration from acetogenesis or waste digestion processes. Acetic acid feed was coupled to the pH sensor and was supplied to maintain a constant pH of the culture optimal for cell growth. Acetic acid thus served as both pH moderator and carbon feedstock. Considering that protonated acetic acid crosses the cellular membrane through passive transport and affects intracellular pH balance (20, 21), the fermentation pH was maintained at 7, which is higher than the pK_a of acetic acid. In this way, acetic acid existed primarily in the salt form, which is less toxic to the cells. The C/N ratio of the feeding liquid was set to 32 for the first 96 h and thereafter only acetic acid was fed. Tangential filtration was applied throughout the whole process with a hollow fiber filter module, such that the working volume within the fermenter was maintained at 1.5 L. Time courses for growth and lipid production are shown in Fig. 2*A*. Acetate concentration decreased to zero starting from 72 h and stayed below 2 g/L afterward, whereas lipids continued to accumulate. However, although the lipid content reached as high as 53%, the overall biomass was only 19 g/L, which showed that cell growth was inhibited to a certain degree.

Careful examination of the fermentation dynamics revealed notable metabolic features, which helped us understand why feeding dilute acetic acid caused only deterioration of growth. The first and most significant factor was the relationship between acetate feed and assimilation. We noted that dilute acetic acid fed in response to pH control was unable to fully compensate for its consumption by the cells. The imbalance between these two factors can be explained by the mechanism of the cell perfusion process, the dissociation equilibrium of acetic acid, and proton balance of the pH-constant fermentation (*Notes on the Effect of Carbon Starvation*). When acetate concentration decreased to 2.5 g/L, the carbon feed rate began to decrease dramatically (Fig. 2*B*), suggesting a decrease in acetate consumption rate. The limitation in carbon supply caused carbon starvation, which slowed down and eventually stopped cell growth and lipid synthesis. This phenomenon indicated that to satisfy the carbon

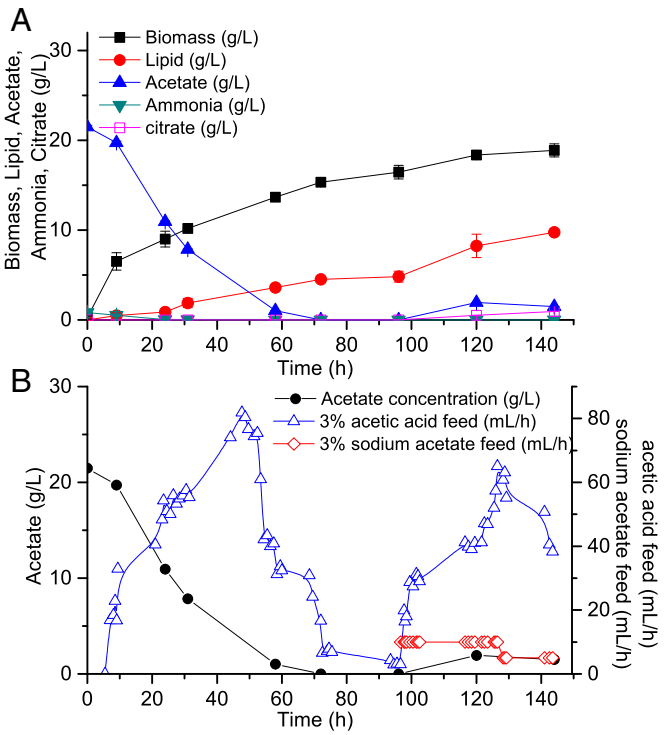

Fig. 2. Lipid production using a carbon-restrained mode by feeding 3% acetic acid. (*A*) Time courses for biomass and lipid production within the bioreactor. (*B*) Time courses for acetic acid concentration as well as acetic acid and acetate (added after 97 h) feed rates.

requirements of the cells, a single-stream feed of acetic acid is inadequate. Therefore, starting from 97 h, we added another feed stream containing 34 g/L sodium acetate at a much lower flow rate (5∼10 mL/h), which was effective in reestablishing the acetate consumption rate to normal levels (Fig. 2*B*). From this, we concluded that an extra dilute acetate feed stream at low flow rates is necessary to avoid carbon starvation when operating under the carbon-restrained mode.

Other factors that affect lipid production include nitrogen supply and the C/N molar ratio. When feeding dilute acetic acid, nitrogen within the reactor is easily exhausted due to consumption by the cells and loss through the permeate. As a result, decelerated cell growth will be observed. Furthermore, the C/N ratio constitutes another important factor that affects carbon flux distribution into either triacylglycerols or by-products, specifically citrate (10, 22, 23). When operating under the carbon-restrained mode established here, minor citrate production is observed when acetate concentration has not yet approached zero but once it has reached zero, citrate production ceases (Fig. S2). This result is a significant improvement over previous carbon-rich cultures where by-production of citrate was observed in the late stage, accounting for more than 10% of the overall lipid titer (11).

Based on these considerations, basic principles for the conversion of dilute acetate into lipids can be drawn: Joint feeding of dilute acetic acid and acetate is required to prevent starvation, sufficient nitrogen should be supplied for cell growth to achieve high titers, and maintaining a reasonable C/N ratio throughout the culture time can minimize by-product formation. Following these principles, we developed a process where 3% acetic acid was fed in cascade with pH control, and ammonium sulfate was fed to keep the C/N feed ratio (acetic acid-derived carbon over ammonium sulfate-derived nitrogen) at 13.2 for the first 72 h and 102 afterward. Feed of 3% sodium acetate was initiated once acetate concentration in the fermenter dropped below 2.5 g/L and its feed rate was manually adjusted, ranging from 2.5 mL/h to ∼20 mL/h according to the acetate consumption rate. Consequently, acetate concentration within the bioreactor approached and stayed at zero starting from 54 h, lipid accumulated throughout the entire culture time, 58 g/L biomass with 57% lipids was obtained with zero citrate by-production, and only 1.9% of the acetate fed was lost from the permeate (Fig. 3). This experiment illustrated the benefits of applying a carbon-restrained mode for lipid overproduction and demonstrated the feasibility of using dilute acetic acid/acetate as the sole carbon source to produce lipids with a comparable titer to that resulting from traditional processes established by feeding concentrated acetic acid.

A Rational Algorithm Design of Carbon Feed Strategies. A joint feeding of acetic acid and acetate was shown to effectively maintain a normal carbon assimilation rate. As such, the feed rate of sodium acetate is critical in determining process performance. Underfeeding will cause carbon starvation, leading to decelerated growth and lipid synthesis, whereas overfeeding will result in a rise of acetate concentration in the fermentation broth, leading to carbon loss from the permeate, citrate by-production, and a decrease in process yield. An optimal carbon feed strategy balancing these two opposing effects can be obtained by two possible rational algorithms that use either off-line periodic measurements or on-line real-time measurements for metabolic activities, respectively.

The first model (Fig. S3) assumed that the cells are at a metabolic steady state during fermentation so that the specific growth rate and substrate consumption rate are approximately constant. This assumption allowed us to predict cell growth and

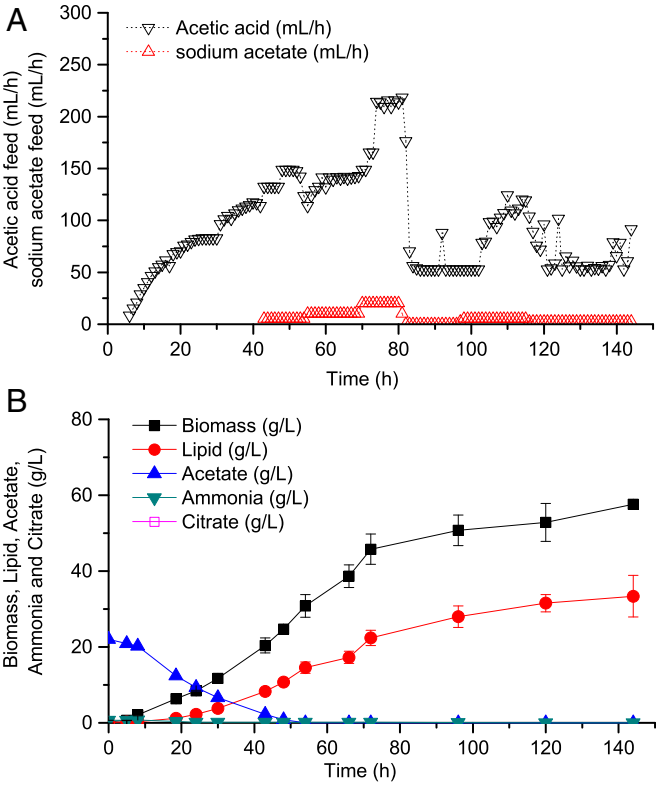

Fig. 3. Lipid production using a joint feeding of 3% acetic acid and sodium acetate. (*A*) Time courses for acetic acid and sodium acetate feed rates. (*B*) Time courses for biomass and lipid production.

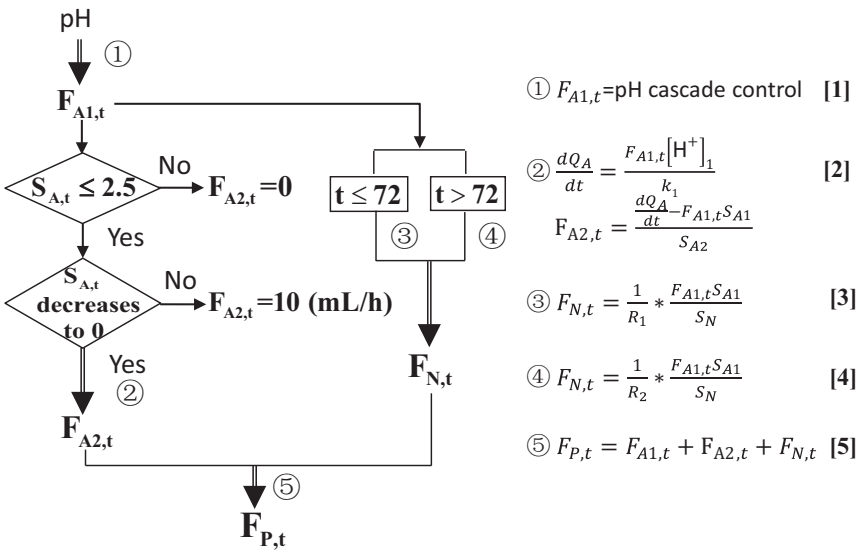

Fig. 4. Model 2 for the joint feeding of 3% acetic acid and sodium acetate based on on-line real-time measurements. Variables used: F_{A1}, instantaneous acetic acid feed rate (mL/h); F_P, instantaneous permeate flow-out rate (mL/h); F_{A2}, instantaneous sodium acetate feed rate (mL/h); F_N, instantaneous ammonium sulfate feed rate (mL/h); $[H^+]_1$, proton concentration in the 3% acetic acid fluid (measured by pH); k_1, coefficient obtained from regression; Q_A, molar amount of acetate consumption (mmol); R_1 and R_2, the C/N ratios for 0–72 h and 72–144 h culture, respectively; S_A, acetate concentration in the reactor (mol/L); S_{A1}, acetic acid feed concentration (0.5 mol/L); S_{A2}, sodium acetate feed concentration (0.5 mol/L); S_N, ammonium concentration in the ammonium sulfate feed stream (0.72 mol/L). $F_{A2} = 10$ when $0 < S_{A,t} < 2.5$ (at this rate, acetate feed cannot compensate for consumption, leading to gradual decrease in acetate concentration within the fermentation broth). $R_1 = 14$ and $R_2 = 100$.

substrate consumption at the next time interval from measurements obtained during the current time period (OD, bioreactor acetate concentration, and permeate volume). From it, the optimal feed rates of acetic acid and sodium acetate can be deduced. By applying this model, we were able to obtain 55 g/L lipids after 144 h of fermentation, and the lipid productivity reached 0.38 $g{\cdot}L^{-1}{\cdot}h^{-1}$ (Fig. S4). These results outcompeted the previously published data (46 g/L lipids in 170 h fermentation), which were the best reported to date (11). Furthermore, our fermentation used only dilute acetate as feed and, more importantly, the carbon-restrained operation eliminated by-product generation (Fig. S4, less than 0.1%, compared with 7.8% in previous studies) and resulted in significantly less acetate loss (lower than 1.5% of total acetate fed). In fact, carbon loss occurred only in the initial stage of fermentation, when acetate concentration was still high in the reactor. Theoretically, this loss can be eliminated in a scaled-up process where cell perfusion can be started after acetate has been depleted. Thus, these results demonstrated the feasibility of fully using dilute acetic acid for lipid production in continuous systems.

This previous model is promising for complete dilute acetic acid utilization. The major drawback, however, is its reliance on frequent sampling of fermentation conditions for the calculated feeding strategy to be accurate, which can be labor intensive. Furthermore, to enable fully automated control, on-line HPLCs or other advanced analytical equipment would be required for the quantification of acetate concentration and these can be difficult to incorporate into industrial-scale bioreactors. Consequently, we further improved the control design to rely on real-time, on-line measurements of pH, as shown in Fig. 4. There are two modifications in this model: First, acetate consumption rate is correlated to acetic acid feed rate (Fig. 4, Eq. **2**), and second, the flow rate of permeate is correlated with the sum of feed-in rates (Fig. 4, Eq. **5**). These two settings ensure that once acetate concentration approaches a set point (which is zero in the current study), by using carbon mass balance, volume balance, and proton balance, the instantaneous feed strategy can be calculated in real time without the need to measure OD and acetate concentration. Overall, this model offered a more precise control of process parameters and thereby lipid productivity was improved significantly as shown in Fig. 5. This feed strategy successfully maintained carbon concentration at zero for 100 h and the cells produced 75 g/L lipid with a productivity of 0.52 $g{\cdot}L^{-1}{\cdot}h^{-1}$. There was negligible citrate by-production, and only 2.6% acetate was

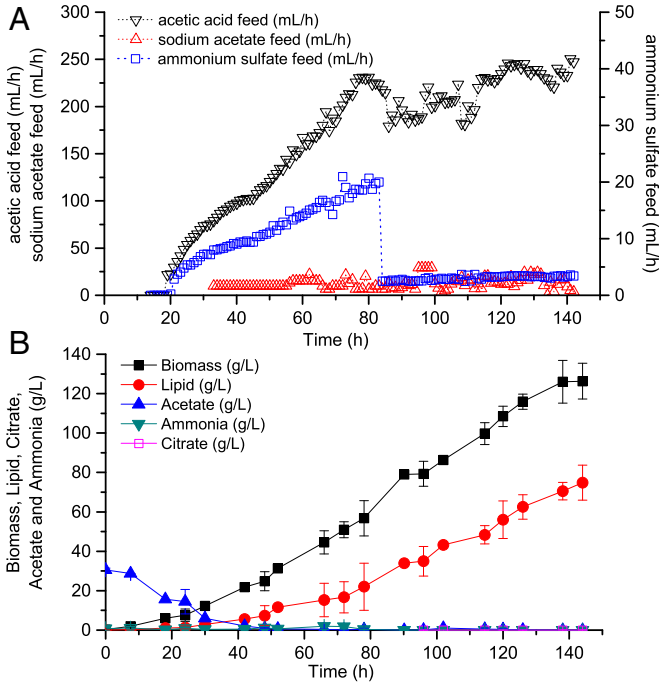

Fig. 5. Lipid production using a carbon-restrained mode by applying model 2. (*A*) Time courses for acetic acid and sodium acetate feed rates. (*B*) Time courses for biomass and lipid production.

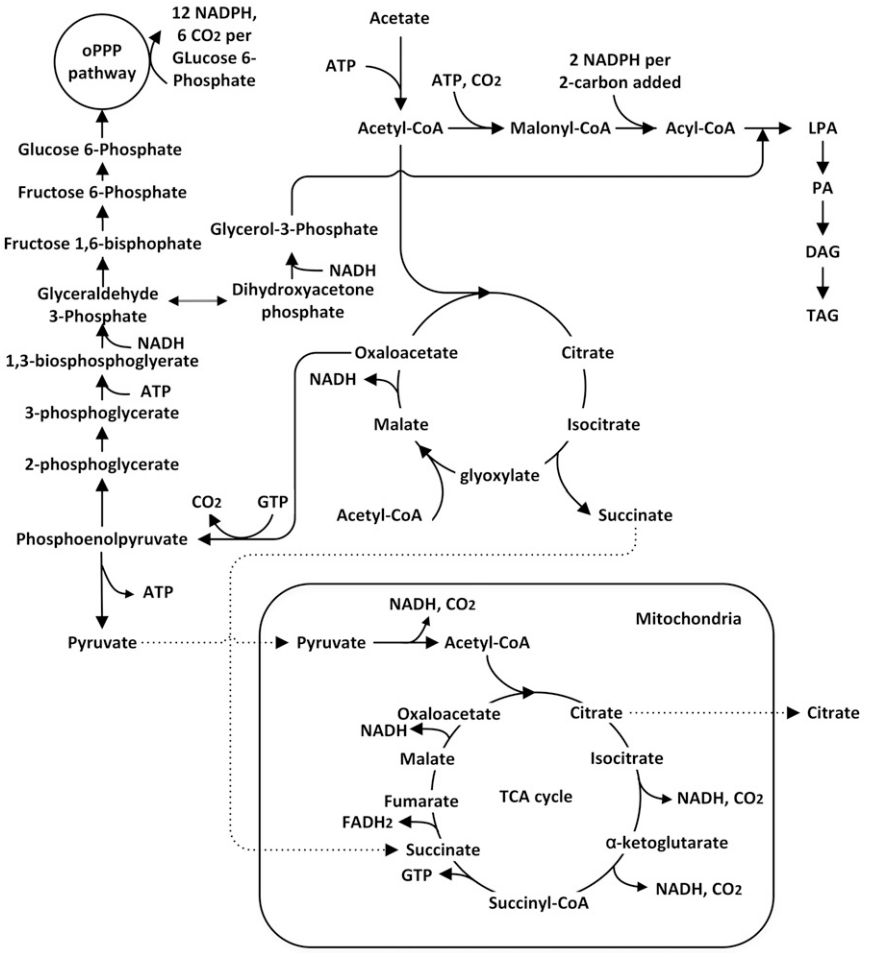

Fig. 6. Metabolic network of lipid synthesis in *Y. lipolytica*. Abbreviations used: DAG, diacylglyceride; LPA, lysophosphatidic acid; oPPP, oxidative pentose phosphate pathway; PA, phosphatidic acid; TAG, triacylglyceride.

lost from the permeate. As a result, the overall lipid yield reached 0.15 g/g, an improvement over model 1.

Optimization of Nitrogen Feed Based on Respiratory Quotient–CO_2 Transfer Rate Feedback Control. Through well-tuned control of acetate feed parameters, the above strategies nearly optimized carbon flux toward lipid synthesis given the requirements for biomass formation and cell maintenance. Further improvement of process performance requires that cell biomass be increased while maintaining the optimal lipid synthesis achieved by the previous controls. To enhance biomass production, more nitrogen must be fed to the reactor but at a rate just enough to supply the needs of cell growth. Otherwise, the C/N ratio may deviate significantly from levels suitable for lipid synthesis. In previous models, nitrogen was fed at a fixed pattern that was correlated to carbon feed, with the C/N ratio maintained at 14 for the first 72 h to support growth and 100 for the next 72 h to support lipid production, as was determined through previous experimental results. However, the optimal set point for nitrogen may vary during the time course of the fermentation. By changing the set point in a dynamic pattern to synchronize with the time-varying nature of the optimum, it is possible to further increase overall lipid yield, titer, and productivity.

To this end, we applied nitrogen feed control in response to the respiratory quotient (RQ) and CO_2 transfer rate (CTR), both of which can be determined from measurements of the bioreactor exhaust gas. Inspecting the metabolism of lipid synthesis in *Y. lipolytica* (Fig. 6) (24, 25) suggests that these two indicators can provide valuable information about the metabolic processes taking place, given the conditions in the culture.

RQ is the ratio of CO_2 evolution rate versus O_2 uptake rate and can be used to determine whether the cells are diverting metabolic flux toward biomass or lipid synthesis. If the cells are using resources for lipid synthesis only, RQ can reach a theoretical maximum of 1.6 (*Notes for Exhaust Gas Analysis*). On the other hand, if cell growth is the primary metabolic activity, RQ will stay below 1.1 (Fig. S5). In addition, because citrate synthesis nets no CO_2 evolution (*Notes for Exhaust Gas Analysis*), a significant decrease in RQ is expected when metabolic flux is diverted to citrate production. Based on these considerations, during lipid production the RQ value is expected to be between 1.1 and 1.6. CTR can also be used as an indicator to probe metabolic activity. The major contribution to CO_2 comes from the oxidative pentose phosphate pathway (PPP) and the tricarboxylic acid (TCA) cycle, which produce NADPH and ATP, respectively, to maintain cellular function and synthesize lipid (Fig. 6). Therefore, a growing trend of CTR is expected during fermentation as long as cell propagation and lipid production are taking place. A plateau will be reached if a metabolic steady state is maintained. However, if there is a major flux diversion toward citrate, CTR will decrease because there will be less flux flowing through the TCA cycle and oxidative PPP, thereby impeding lipid synthesis due to the lack of ATP and NADPH. Based on

this consideration, the trend of CTR can be used as the second indicator to probe citrate by-production.

Combined analysis of RQ and CTR can be used to adjust feed rates of nitrogen. Before *Y. lipolytica* entered the lipid overproduction phase (RQ < 1.2), nitrogen was fed at a constant rate to accumulate biomass as quickly as possible. Once RQ reached a certain threshold, nitrogen feed was calculated according to the RQ-CTR feedback control algorithm, with the purpose of maintaining a fermentation condition favorable to lipid overproduction while still sustaining biomass synthesis. Coupled to the previous acetate feed model (Fig. 4), we have designed a process that applied both optimized carbon and nitrogen feed strategies based on on-line real-time indicators (Fig. 7). With this control, acetic acid and ammonium sulfate feed were correlated with one another and could both respond to the instantaneous fluctuations of cellular metabolic activities, leading to a significant boost in cell growth and lipid accumulation (Fig. 8). After 144 h, the final biomass, lipid titer, and lipid productivity achieved 194 g/L, 115 g/L, and 0.80 $g{\cdot}L^{-1}{\cdot}h^{-1}$, respectively, which represents a more than twofold improvement over the currently best reported results. With the closed-loop control, more nitrogen was used for cell growth in later stages without limiting lipid synthesis and in turn the increased biomass boosted carbon assimilation (only 1.9% carbon loss) as well as lipid production. In addition, throughout the entire fermentation process, cell metabolism was well under control to avoid citrate production, resulting in nearly zero citrate concentrations. Instantaneous lipid yield was sustained above 0.15 g/g for upward of 100 h, and the overall lipid yield is 0.16 g/g, which is very close to the theoretical maximum of 0.167 (*Notes on Stoichiometry Analysis of Lipid Production on Acetate*), suggesting that the potential of lipid overproduction in *Y. lipolytica* has been fully displayed.

Conclusions

This work demonstrated the feasibility of fully using dilute acetic acid/acetate as the sole carbon source, achieving superior lipid titer (115 g/L) and productivity (0.8 $g{\cdot}L^{-1}{\cdot}h^{-1}$). Compared with previously reported data for best performance obtained from the carbon-rich fermentation mode (11), our results represent a 150% increase in lipid titer and a 196% increase in lipid productivity. In fact, the achieved productivity is now equivalent to that of high-strength glucose-based cultures (26). Table 1 summarizes the fermentation performance under the carbon-restrained mode we have established with the different feed strategies described in this work. It illustrates the benefits of a rational feed control design that is able to optimize the biological activity of the cells through control of culture conditions. This rational design process is appealing in several respects.

First, it demonstrates the possibility of applying a carbon-restrained mode for high-density cell culture and lipid production. Substrates were continuously fed into the fermenter and fully converted into valuable products with negligible loss through the permeate stream. The efficiency of such a system stems from balancing carbon feed with the metabolic demand, such that the substrate concentration can be maintained at zero in the reactor without inhibiting cell growth and lipid synthesis. This concept is widely applicable to other systems as well, especially those

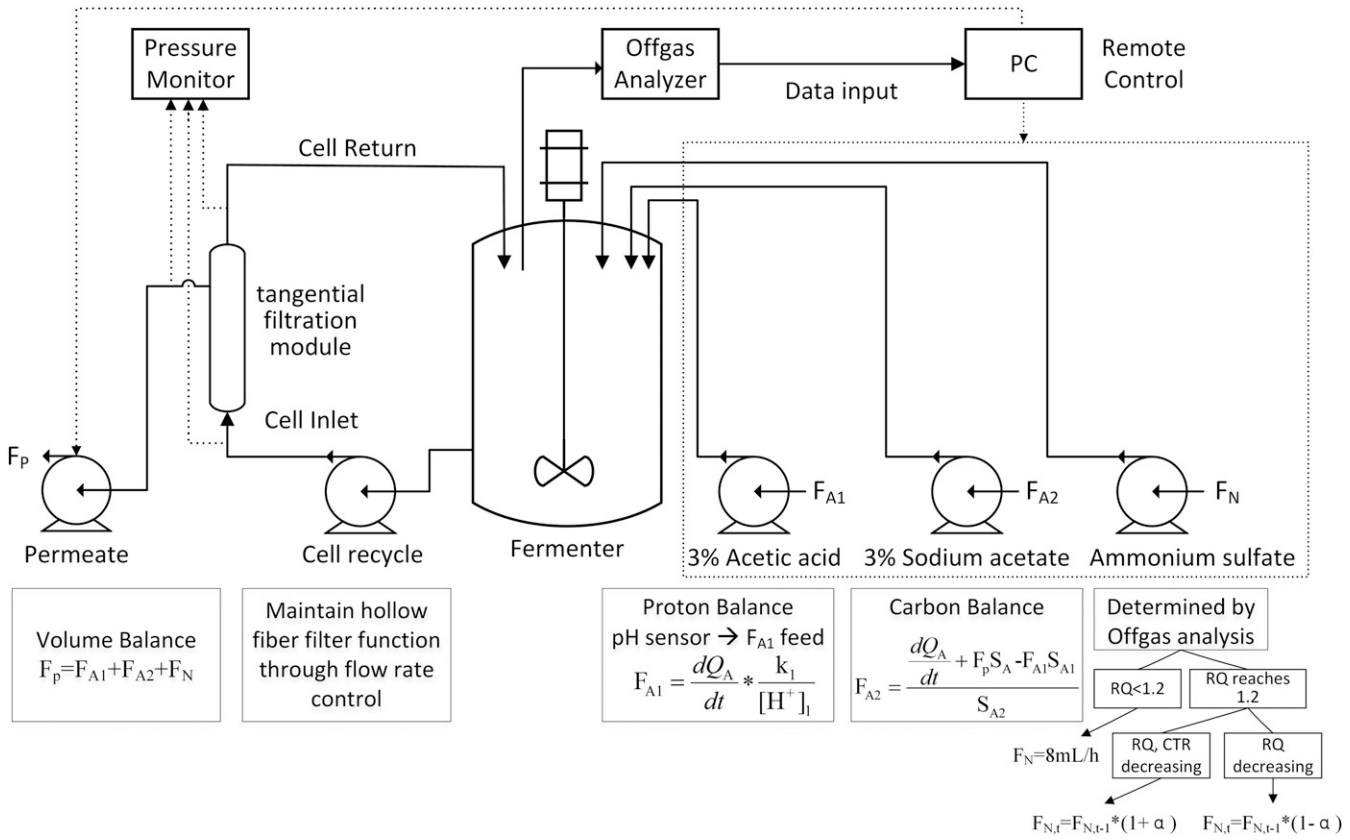

Fig. 7. Optimized process design for lipid production using model 3. This diagram shows the rational design of carbon and nitrogen feed when acetate concentration is maintained at zero in the system. RQ threshold is set at 1.2 to trigger the start of RQ and CTR feedback control. Decrease in RQ implies only an insufficient lipid synthesis, indicating a nitrogen overfeed, whereas decrease in both RQ and CTR implies a flux diversion toward undesired pathways, indicating the need for an increased nitrogen feed. $\alpha = 0.05$.

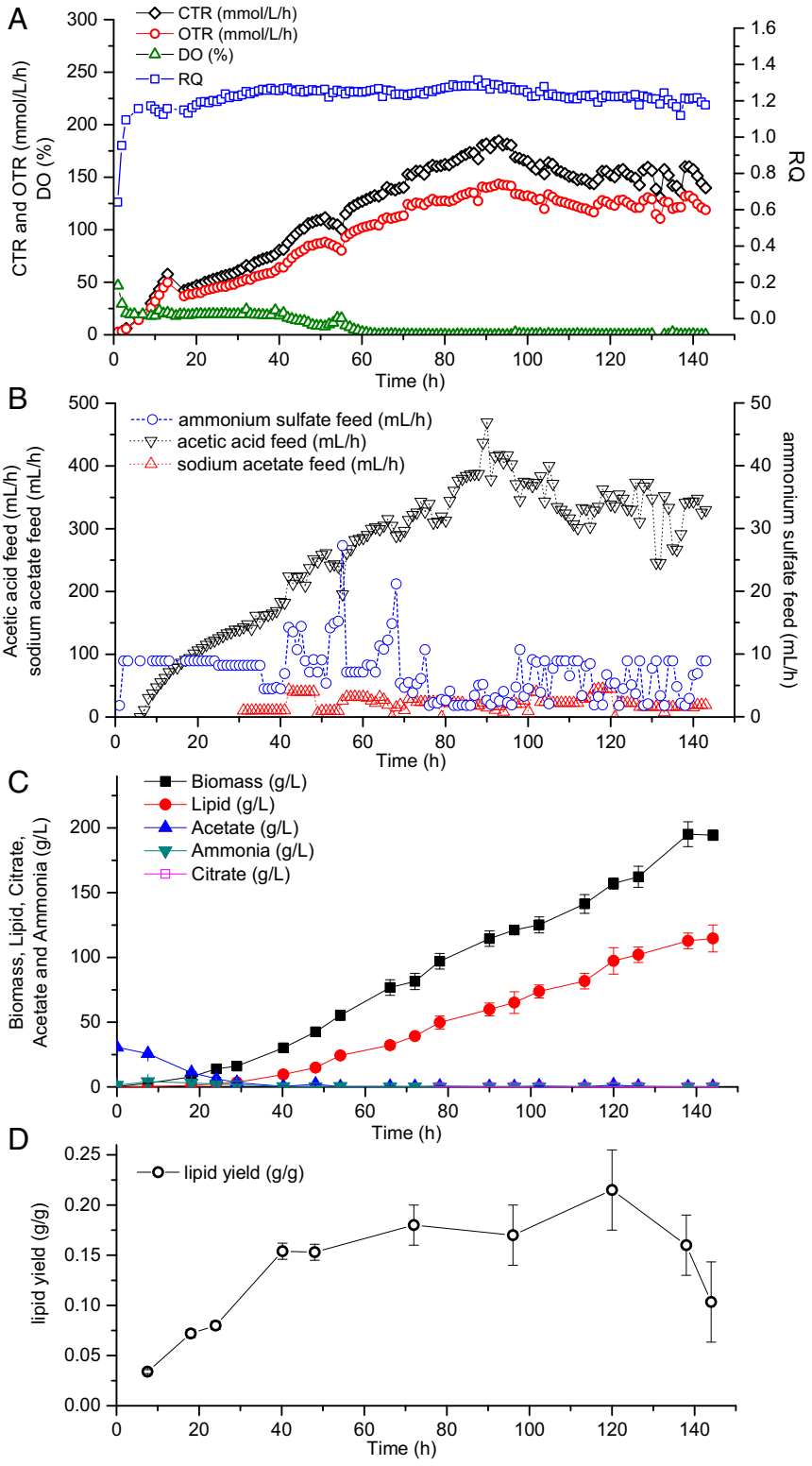

Fig. 8. Lipid production using the well-tuned carbon and nitrogen control strategies. (*A*) On-line exhaust gas analysis. (*B*) Time courses for carbon and nitrogen feed rates. (*C*) Time courses for lipid and biomass production. (*D*) Instantaneous yield on acetate over time.

designed to biologically convert resource streams containing low-strength organic nutrients into value-added products.

Second, the control algorithm for carbon and nitrogen feeding requires only basic principles. Proton balance, carbon mass balance, and volume balance were used to determine carbon feed strategy whereas qualitative relationships between metabolic activity and exhaust gas measurements were used to determine nitrogen feed strategy. No complex mathematical models or estimation algorithms are required and thus our model is relatively robust against errors and sensitivity problems.

Table 1. Lipid production through carbon-restrained mode by applying different feed strategies

Biomass, g/L	Lipid, g/L	Citrate, g/g biomass	Lipid yield, g/g	Lipid productivity, $g \cdot L^{-1} \cdot h^{-1}$	Acetate loss, %	Feed strategies
19 ± 0.7	10 ± 0.3	0.082 ± 0.002	0.09 ± 0.01	0.07 ± 0.00	6.8 ± 0.0	3% acetic acid feed
58 ± 0.8	33 ± 5.0	0.000 ± 0.000	0.14 ± 0.01	0.23 ± 0.03	1.9 ± 0.0	Joint feed of 3% acetic acid and acetate
93 ± 2.4	55 ± 3.7	0.001 ± 0.000	0.14 ± 0.00	0.38 ± 0.03	1.5 ± 0.0	Joint feed of 3% acetic acid and acetate by applying model 1
127 ± 9.1	75 ± 8.9	0.003 ± 0.001	0.15 ± 0.02	0.52 ± 0.07	2.6 ± 0.1	Joint feed of 3% acetic acid and acetate by applying model 2
194 ± 4.0	115 ± 10.4	0.001 ± 0.000	0.16 ± 0.00	0.80 ± 0.08	1.9 ± 0.4	Optimized carbon and nitrogen feed by applying model 3

Finally, the input variables to the model, which include pH, feeding rate, RQ, and CTR, can all be measured directly online with readily available equipment. Labor-intensive sampling is eliminated and the control schemes can be easily implemented in existing large-scale bioreactors, both of which are ideal for industrial applications. More importantly, the design of our system allows the probing of instantaneous metabolic activities within the culture, enabling real-time feedback control loops to maintain operating conditions at an optimum. Oftentimes this approach can be much more advantageous compared with processes based on intermittent sampling and parameter adjustment.

In summary, with our rationally designed fermentation control system, low-strength acetic acid derived from biological CO_2 fixation, municipal/industrial waste streams, and lignocellulosic biomass pyrolysis can be processed continuously at large amounts, resulting in high lipid titers at yields very close to the theoretical maximum and productivities matching those obtained in glucose fermentations. Such a process leverages the potential of low-cost dilute feedstocks that were previously difficult to use to be fully converted into microbial lipids used for transportation fuels.

Materials and Methods

Strain and Culture Conditions. The strain used in the present study was a previously engineered lipid-overproducing strain of *Y. lipolytica*, MTYL065, which overexpresses acetyl-CoA carboxylase 1 (*ACC1*) and diacylglycerol acyltransferase 1 (*DGA1*) (10). The enzymes encoded by these two genes catalyze the first and last steps of TAG synthesis, respectively, thereby greatly enhancing the flux through this pathway.

The strain was maintained on minimal media plates containing 20 g/L glucose, 5 g/L ammonium sulfate, and 1.7 g/L yeast nitrogen base without amino acids and ammonium sulfate (YNB −AA −AS) and stored at 4 °C. For inoculum preparation, *Y. lipolytica* was precultured in a 14-mL culture tube containing 3 mL yeast extract–peptone–dextrose (20 g/L glucose, 20 g/L peptone, and 10 g/L yeast extract). After 24 h, 1 mL of the tube culture was transferred to a 250-mL flask with 50 mL working volume containing yeast extract–peptone–acetate (28 g/L sodium acetate, 20 g/L peptone, and 10 g/L yeast extract). Two shake flask cultures were inoculated per tube culture. All tube and shake flask cultures were incubated at 30 °C and 250 rpm (New Brunswick Innova 43).

After 24 h, the two shake flask cultures were used to inoculate a 2-L stirred tank reactor (New Brunswick Scientific) to an initial OD_{600} of 1.0. For all bioreactor cultures, the working volume was 1.5 L, aeration rate was 2 volume of air per volume of culture per minute (vvm), The dissolved oxygen (DO) setpoint was 20%, and agitation was within the range of 250~800 rpm in cascade with DO measurements. For detailed culture conditions, see *Notes for Materials and Methods*.

Tangential Flow Filtration System for Cell Recycling. The system consisted of a hollow-fiber filter module (pore rating, 0.2 μm; surface area, 470 cm^2) (Minicros Sampler; Spectrum Laboratories), two digital pumps (Masterflex), a digital pressure monitor (KrosFlo; Spectrum Laboratories), and required tubing connections. The hollow-fiber filter module was used to recycle cells and remove excess volume pumped into the reactor through the feeding streams. The inlet of the filter module was connected to the reactor via a digital pump, which drove cell recycling and filtration at a flow rate ranging from 3,000 mL/h to ~10,000 mL/h. The permeate flow was driven by the second pump at a flow rate equal to the total feed-in rates of the feeding streams. The pressure monitor showed the instantaneous pressures of the inlet, retentate, permeate, and transmembrane streams, which indicated membrane integrity and filtration status.

Exhaust Gas Analysis. Oxygen and carbon dioxide content in the exhaust gas was analyzed by an off-gas analyzer (DASGIP GA1; Eppendorf). The integrated mass flow sensors in the analyzer enabled automatic calculation of oxygen transfer rate (OTR), CTR, and RQ, according to the equations

$$\mathrm{OTR} = \frac{Q_{\mathrm{air}}}{V_L V_N} * \left[X_{O_2,\mathrm{in}} - X_{O_2,\mathrm{out}} \left(\frac{1 - X_{CO_2,\mathrm{in}} - X_{O_2,\mathrm{in}} - X_{H_2O,\mathrm{in}}}{1 - X_{CO_2,\mathrm{out}} - X_{O_2,\mathrm{out}} - X_{H_2O,\mathrm{out}}} \right) \right]$$

$$\mathrm{CTR} = \frac{Q_{\mathrm{air}}}{V_L V_N} * \left[X_{CO_2,\mathrm{out}} - X_{CO_2,\mathrm{in}} \left(\frac{1 - X_{CO_2,\mathrm{in}} - X_{O_2,\mathrm{in}} - X_{H_2O,\mathrm{in}}}{1 - X_{CO_2,\mathrm{out}} - X_{O_2,\mathrm{out}} - X_{H_2O,\mathrm{out}}} \right) \right]$$

$$\mathrm{RQ} = \frac{\mathrm{CTR}}{\mathrm{OTR}},$$

where Q_{air} is the airflow rate (L/h); V_L is the liquid volume (L); V_N is the volume of 1 mol gas under normal conditions (22.4 L/mol); and $X_{O_2,\mathrm{in}}$, $X_{CO_2,\mathrm{in}}$, $X_{H_2O,\mathrm{in}}$, $X_{O_2,\mathrm{out}}$, $X_{CO_2,\mathrm{out}}$, and $X_{H_2O,\mathrm{out}}$ are mole fractions of gas composition in the fresh and exhaust air ($X_{O_2,\mathrm{in}}$ = 20.95%, $X_{CO_2,\mathrm{in}}$ = 0.03%).

Real-time records of respiratory measurement and calculation results were imported into BioCommand Batch Control (Version 2010; New Brunswick Scientific) for the feedback control model. In this model, OTR and CTR data were smoothed by a second-order Butterworth digital filter (cutoff frequency 0.05), using the BioCommand software program. The trend of CTR was determined by applying a linear regression analysis to a moving data window containing the most recent 15 min of filtered data at a sampling rate of 1 min^{-1}. The trend of RQ was determined by comparing the mean value of the most recent 15 min of RQ data at a sampling rate of 1 min^{-1} with a threshold value (the maximum RQ achieved in the fermentation process). The trends were then passed on to the control algorithm for evaluation of the metabolic status and subsequent control actions.

Quantification of Dry Cell Weight, Extracellular Metabolite, and Lipids. Dry cell weight (DCW) was measured by sampling 1 mL of the fermentation broth from the reactor. Samples were centrifuged at 18,000 × *g* for 10 min, washed with deionized water, and dried at 60 °C until a constant weight was reached.

Extracellular acetate and citrate concentrations were quantified using high-performance liquid chromatography (HPLC). One milliliter of culture was extracted from the bioreactor and then centrifuged at 18,000 × *g* for 10 min. The supernatant was retained and filtered through 0.2-μm nylon syringe filters (Denville Scientific Inc.). An Agilent 1200 HPLC system (Bio-Rad HPX-87 H column) coupled to a G1362A refractive index detector was used for analysis. A total of 14 mM sulfuric acid was used as the mobile phase, flowing at a rate of 0.7 mL/min. The injection volume was 10 μL. The extracellular concentration of ammonium sulfate was measured using an ammonium assay kit (Sigma-Aldrich).

Lipids synthesized by *Y. lipolytica* were quantified using gas chromatography coupled to a flame ionization detector (GC-FID). A 0.1- to 1-mL sample was extracted from the bioreactor such that it contained ~1 mg dry cells. Samples were centrifuged at 18,000 × *g* for 10 min and the supernatant was discarded. A total of 100 μL internal standard containing 2 mg/mL methyl tridecanoate (Sigma-Aldrich) and 2 mg/mL glyceryl triheptadecanoate (Sigma-Aldrich) dissolved in hexane was added to each sample as an internal standard. Methyl tridecanoate was used for volume loss correction during sample preparation and glyceryl triheptadecanoate was used for transesterification efficiency correction. A total of 500 μL 0.5 N sodium methoxide

(20 g/L sodium hydroxide in anhydrous methanol) was then added for transesterification into fatty acid methyl esters (FAMEs) and the reaction was allowed to proceed for 60 min through vortexing at 1,200 rpm (VWR vortex mixer). Afterward, 40 μL of 98% sulfuric acid was added to neutralize the pH. A total of 500 μL hexane was added to each sample and vortexing for 30 min at 1,200 rpm (VWR vortex mixer) was performed for FAME extraction. The top hexane layer containing the FAMEs was used for analysis after centrifugation at 6,000 × *g* for 1 min. An Agilent J&W HPINNOWax capillary column mounted to a Bruker 450-GC system was used for separation of the FAME species. The injection volume was 1 μL, split ratio was 10, and injection temperature was 260 °C. The column was held at a constant temperature of 200 °C and helium was used as the carrier gas with a flow rate of 1.5 mL/min. The FID was set at a temperature of 260 °C with the flow rates of helium make-up gas, hydrogen, and air at 25 mL/min, 30 mL/min, and 300 mL/min, respectively. All experiments were performed in triplicate and the average and SD were presented for data analysis.

ACKNOWLEDGMENTS. This research was supported by Department of Energy's Genomic Science Program Grant DE-SC0008744 (MIT: 692-6611). We also thank the China Scholarship Council for financial support.

1. Pfleger BF (2016) Microbes paired for biological gas-to-liquids (Bio-GTL) process. *Proc Natl Acad Sci USA* 113:3717–3719.
2. Higman C (2016) State of the gasification industry: Worldwide gasification and syngas databases 2016 update. Available at www.gasification-syngas.org/uploads/downloads/2016-presentations/2016-Wed-Higman.pdf. Accessed June 8, 2017.
3. Dahmen N, Henrich E, Dinjus E, Weirich F (2012) The bioliq bioslurry gasification process for the production of biosynfuels, organic chemicals, and energy. *Energy Sustain Soc* 2:1–44.
4. Molitor B, et al. (2016) Carbon recovery by fermentation of CO-rich off gases - Turning steel mills into biorefineries. *Bioresour Technol* 215:386–396.
5. Romero M, Steinfeld A (2012) Concentrating solar thermal power and thermochemical fuels. *Energy Environ Sci* 5:9234–9245.
6. Ragsdale SW, Pierce E (2008) Acetogenesis and the Wood-Ljungdahl pathway of CO(2) fixation. *Biochim Biophys Acta* 1784:1873–1898.
7. Bengelsdorf FR, Straub M, Dürre P (2013) Bacterial synthesis gas (syngas) fermentation. *Environ Technol* 34:1639–1651.
8. Lian J, Garcia-Perez M, Coates R, Wu H, Chen S (2012) Yeast fermentation of carboxylic acids obtained from pyrolytic aqueous phases for lipid production. *Bioresour Technol* 118:177–186.
9. Jiang J, et al. (2013) Volatile fatty acids production from food waste: Effects of pH, temperature, and organic loading rate. *Bioresour Technol* 143:525–530.
10. Tai M, Stephanopoulos G (2013) Engineering the push and pull of lipid biosynthesis in oleaginous yeast Yarrowia lipolytica for biofuel production. *Metab Eng* 15:1–9.
11. Hu P, et al. (2016) Integrated bioprocess for conversion of gaseous substrates to liquids. *Proc Natl Acad Sci USA* 113:3773–3778.
12. Wood D, Nwaoha C, Towler B (2012) Gas-to-liquids (GTL): A review of an industry offering several routes for monetizing natural gas. *J Nat Gas Sci Eng* 9:196–208.
13. Kennes D, Abubackar H, Diaz M, Veiga M, Kennes C (2016) Bioethanol production from biomass: Carbonhydrates vs syngas fermentation. *J Chem Technol Biotechnol* 91:304–317.
14. Hu P, Rismani-Yazdi H, Stephanopoulos G (2013) Anaerobic CO2 fixation by the acetogenic bacterium *Moorella thermoacetica*. *AIChE J* 59:3176–3183.
15. Gong Z, et al. (2015) Efficient conversion of acetate into lipids by the oleaginous yeast *Cryptococcus curvatus*. *Biotechnol Biofuels* 8:189.
16. Chi Z, Zheng Y, Ma J, Chen S (2011) Oleaginous yeast *Cryptococcus curvatus* culture with dark fermentation hydrogen production effluent as feedstock for microbial lipid production. *Int J Hydrogen Energy* 36:9542–9550.
17. Béligon V, et al. (2015) Improvement and modeling of culture parameters to enhance biomass and lipid production by the oleaginous yeast *Cryptococcus curvatus* grown on acetate. *Bioresour Technol* 192:582–591.
18. Huang XF, et al. (2016) Culture strategies for lipid production using acetic acid as sole carbon source by *Rhodosporidium toruloides*. *Bioresour Technol* 206:141–149.
19. Andersen SJ, et al. (2014) Electrolytic membrane extraction enables production of fine chemicals from biorefinery sidestreams. *Environ Sci Technol* 48:7135–7142.
20. Mondala A, et al. (2011) Effect of acetic acid on lipid accumulation by glucose-fed activated sludge cultures. *J Chem Technol Biotechnol* 87:33–41.
21. Huang C, et al. (2012) Effect of organic acids on the growth and lipid accumulation of oleaginous yeast *Trichosporon fermentans*. *Biotechnol Biofuels* 5:4.
22. Beopoulos A, et al. (2009) Yarrowia lipolytica as a model for bio-oil production. *Prog Lipid Res* 48:375–387.
23. Papanikolaou S, Aggelis G (2009) Biotechnological valorization of biodiesel derived glycerol waste through production of single cell oil and citric acid by *Yarrowia lipolytica*. *Lipid Technol* 21:83–87.
24. Berg J, Tymoczko J, Stryer L (2012) *Biochemistry* (Freeman, New York), 17th Ed.
25. Liu N, Qiao K, Stephanopoulos G (2016) (13)C metabolic flux analysis of acetate conversion to lipids by Yarrowia lipolytica. *Metab Eng* 38:86–97.
26. Qiao K, et al. (2015) Engineering lipid overproduction in the oleaginous yeast *Yarrowia lipolytica*. *Metab Eng* 29:56–65.
27. von Stockar U, Liu J (1999) Does microbial life always feed on negative entropy? Thermodynamic analysis of microbial growth. *Biochim Biophys Acta* 1412:191–211.
28. Jogl G, Tong L (2004) Crystal structure of yeast acetyl-coenzyme A synthetase in complex with AMP. *Biochemistry* 43:1425–1431.